Role of Oxygen Availability in CFTR Expression and Function

Jennifer S. Guimbellot[1,7], James A. Fortenberry[7], Gene P. Siegal[4,5,6], Bryan Moore[8], Hui Wen[7], Charles Venglarik[7], Yiu-Fai Chen[2], Suzanne Oparil[2], Eric J. Sorscher[1,2,3,7], and Jeong S. Hong[4,7]

Departments of [1]Genetics, [2]Medicine, [3]Physiology and Biophysics, [4]Cell Biology, [5]Pathology, [6]Surgery, [7]Gregory Fleming James Cystic Fibrosis Research Center, University of Alabama at Birmingham, Birmingham, Alabama; and [8]Motorola Life Sciences, Northbrook, Illinois

The cystic fibrosis transmembrane conductance regulator (CFTR) serves a pivotal role in normal epithelial homeostasis; its absence leads to destruction of exocrine tissues, including those of the gastrointestinal tract and lung. Acute regulation of CFTR protein in response to environmental stimuli occurs at several levels (e.g., ion channel phosphorylation, ATP hydrolysis, apical membrane recycling). However, less information is available concerning the regulatory pathways that control levels of CFTR mRNA. In the present study, we investigated regulation of CFTR mRNA during oxygen restriction, examined effects of hypoxic signaling on chloride transport across cell monolayers, and related these findings to a possible role in the pathogenesis of chronic hypoxic lung disease. CFTR mRNA, protein, and function were robustly and reversibly altered in human cells in relation to hypoxia. In mice subjected to low oxygen *in vivo*, CFTR mRNA expression in airways, gastrointestinal tissues, and liver was repressed. CFTR mRNA expression was also diminished in pulmonary tissues taken from hypoxemic subjects at the time of lung transplantation. Environmental factors that induce hypoxic signaling regulate CFTR mRNA and epithelial Cl^- transport *in vitro* and *in vivo*.

Keywords: cystic fibrosis transmembrane conductance regulator; hypoxia; cystic fibrosis

Cystic fibrosis (CF) is caused by mutations in the cystic fibrosis transmembrane conductance regulator (CFTR), and results in altered chloride transport in multiple organs. Pulmonary manifestations may begin prenatally, affecting surface airway epithelia and submucosal glands. Viscous secretions obstruct pulmonary glands and bronchi, inhibit mucociliary clearance and oxygen delivery, and promote colonization by bacterial pathogens (1). Chronic suppurative infection further impedes access of the conducting airway epithelium to oxygen by plastering thick, necrotic secretions onto the surface of the airway mucosa, resulting in poor tissue oxygenation that approaches anaerobic conditions (2).

Reduced oxygen tension influences the rate of decline in CF lung disease. Growth and phenotype of *Pseudomonas aeruginosa* is affected by oxygen gradients in the thick mucus layers overlying airway surface epithelium (2). Bacteria penetrate mucus plugs and respond to reduced oxygen by increasing production of capsular polysaccharide, which contributes to proliferation and persistence of bacterial macrocolonies (biofilms).

Hypoxia occurs in airway epithelium in a number of chronic obstructive lung diseases and could have pronounced effects on numerous genes, but has not been adequately investigated either from the standpoint of CFTR transcription or protein expression. In pulmonary vasculature, lung damage conferred by low oxygen *in vivo* is well established (e.g., maladaptive vascular remodeling) (3, 4). Messenger RNA and protein encoded by genes induced by hypoxia, such as vascular endothelial growth factor (VEGF) and platelet-derived growth factor B, are elevated after oxygen deprivation in murine lungs (5, 6). The same is true of alveolar epithelium (7) and numerous cultured pulmonary cell types (including bronchial epithelium) after oxygen deprivation (8). Having said this, very little is known regarding the influence of hypoxia on epithelial genes such as CFTR, and a transcriptome-wide analysis of hypoxia in secretory epithelium has not been conducted previously. Moreover, the pathways by which hypoxia regulates gene expression in epithelial cells are not well characterized. One mechanism that confers a cellular hypoxic response is hypoxia-inducible factor (HIF)-1α, a potent transcriptional stimulatory factor. However, the influence of HIF on CFTR expression or function has not been studied previously, and the extent of hypoxia-induced gene repression (as opposed to mRNA induction) is poorly understood. The present study was therefore designed to investigate an observation that hypoxic signaling leads to pronounced repression of CFTR mRNA, protein, and function. Our findings point to a novel mechanism of regulation pertinent to CFTR transcriptional control and cystic fibrosis disease progression.

CLINICAL RELEVANCE

These findings will be of interest to colleagues studying cystic fibrosis transmembrane conductance regulator biology and maturational processing, ion transport physiology, tissue hypoxia, transcriptional regulation of gene expression, and both inherited and acquired forms of lung disease.

MATERIALS AND METHODS

Cell Lines and Culture Conditions

HT29 (HTB-38) and Calu-3 (HTB-55) cell lines were obtained from ATCC (Manassas, VA) and seeded on 6.5- or 12-mm diameter Transwell filters (Corning-Costar, Corning, NY). Cells were cultured in media (HT29: McCoy's 5a medium supplemented with 7% fetal bovine serum [FBS]; Calu-3: MEM supplemented with 1.0 mM sodium pyruvate, 0.1 mM nonessential amino acids, 1.5 g/L sodium bicarbonate, and 7% FBS) for 4 to 6 days (media bathing both the apical and basolateral compartments) at 37°C in 5% CO_2/95% air. Under these conditions, cells form polarized monolayers with transepithelial resistances greater than 500 $\Omega \cdot cm^2$. In some monolayers, medium was removed from the apical surface to expose cells to air (air/liquid interface, A/L). As a test for effects specifically caused by hypoxic signaling, five different conditions were examined: (*1*) submerging the apical compartment with deep culture medium ($\sim$ 1 cm; liquid/liquid interface, L/L) to limit access to

(*Received in original form December 14, 2007 and in final form April 14, 2008*)

This work was supported by grants from the National Institutes of Health (P50 DK053090) and from the Cystic Fibrosis Foundation (R464) (to E.J.S.).

Correspondence and requests for reprints should be addressed to Jeong S. Hong, Ph.D., 1918 University Boulevard (MCLM 766), Birmingham, AL 35294-0005. E-mail: jhong@uab.edu

Am J Respir Cell Mol Biol Vol 39. pp 514–521, 2008
Originally Published in Press as DOI: 10.1165/rcmb.2007-0452OC on May 12, 2008
Internet address: www.atsjournals.org

oxygen (9–15); (*2*) exposure to 1% O_2/5% CO_2 (balance consisting of N_2) in a tightly sealed modular incubator chamber (Billups-Rothenberg, Del Mar, CA) for 24 to 48 hours at 37°C; (*3*) treatment with dimethyloxalylglycine (DMOG) to specifically block prolyl hydroxylation, and therefore lead to HIF-1α accumulation; (*4*) treatment with cobalt chloride ($CoCl_2$), a hypoxia mimetic; and (*5*) combinations of the above conditions as a means of testing for additive or synergistic effects. The cells were incubated in media containing 3% FBS for a minimum of 24 hours before each experiment.

Reagents

$CoCl_2$ hexahydrate was purchased from Sigma-Aldrich (St. Louis, MO) and dissolved in media at stock concentration of 5 mM. DMOG was purchased from Frontier Scientific, Inc. (Logan, UT) and dissolved in media at 500 mM. $CoCl_2$ and DMOG were added to the basolateral cell surface (final concentrations, 100 μM and 2 mM, respectively).

Microarray

Total RNA was purified from HT29 cells (QiaAmp RNeasy kit per manufacturer instructions [Qiagen, Valencia, CA]), and RNA quality was assessed (2100 Bioanalyzer; Agilent, Palo Alto, CA). Briefly, the RNA was processed as previously described (16, 17). A reaction mix containing 5 μg of total RNA, bacterial RNA controls, 0.5 pmol/μl T7-(dT)24 oligonucleotide primers, and SuperscriptTM II reverse transcriptase (200 U/ml; Invitrogen, Carlsbad, CA) was incubated at 42°C for 1 hour. Second-strand cDNA was generated with *Escherichia coli* DNA polymerase I (40 U; Invitrogen) in the presence of 2 U RNase H for 2 hours at 16°C. The resulting cDNA was purified and added to an *in vitro* transcription reaction containing buffer, ATP, GTP, CTP, biotin 11-UTP (Ambion, TX), and enzyme mix. The reaction was incubated at 37°C for 14 hours followed by antisense RNA (aRNA) purification (RNeasy kit; Qiagen). Ultraviolet absorbance was measured at 260 nm to quantitate aRNA. The aRNA was fragmented and hybridized to a Codelink (GE Medical, Piscataway, NJ) Uniset Human I Expression Bioarray. This array contains 9,589 30-mer oligonucleotide probes designed to 9,203 unique accession numbers including 386 control probes on a three-dimensional polymeric surface. After overnight incubation, the hybridized transcripts were detected with streptavidin–Alexa 647 conjugates (Invitrogen), and scanned on a GenPix Scanner (Axon Corp, Sunnyvale, CA) at a PMT voltage of 600 and 10 μm resolution, and data analyzed with Codelink Data analysis software. Three additional sets of mRNA expression array were performed to confirm the data using Affymatrix human genome U133 plus 2.0 arrays. The raw data set is available from the Gene Expression Omnibus under accession GSE9234. The chip array was repeated with modifications a total of four independent runs, with confirmation of the findings shown in the present study. Positions of interest noted during the gene chip analysis (e.g., CFTR) were validated by semi-quantitative RT-PCR, quantitative real-time (fluorescein-based) PCR, protein measurements, and biophysical assays of CFTR chloride transport.

Semiquantitative RT-PCR

Relative quantitation of CFTR mRNA was performed with a one-step RT-PCR kit (Qiagen) using total RNA as the template. Primer sequences used for CFTR mRNA were ACTTCACTTCTAATGATGAT and AAAACATCTAGGTATCCAA; for β-actin, ACACTGTGCC CATCTACGAGG and AGGGGCCGGACTCGTCATACT; for GA PDH, TCGTGGAAGGACTCATGACC and TCACCACCCTGTT GCTGTA; and for VEGF, AGAATCATCACGAAGTGGTGAA and AAGGCCCACAGGGATTTTCTTG. RT-PCR was performed as described in the technical manual (Qiagen) with 27 cycles of amplification.

Fluorescence-Based Real-Time RT-PCR

Cftr mRNA levels were assessed by fluorescence-based kinetic real-time RT-PCR using the ABI PRISM 7500 Sequence Detection System (Applied Biosystems, Inc., Foster City, CA). One-step RT-PCR was conducted on six serial dilutions of RNA isolates using One-Step RT-PCR Master Mix Reagent kit and Assays-on-Demand Gene Expression Probes (CFTR Assay ID: HS00357011_m1, FAM/MGB; Applied Biosystems) and eukaryotic 18S rRNA (RT-PCR endogenous control). All *cftr* values were normalized to 18S rRNA (from the same sample) according to the Applied Biosystems relative quantification method as described in ABI manual, as a means of establishing specific changes in CFTR mRNA levels as opposed to more general effects on cellular transcription.

Detection of HIF-1α by Western Blotting

Protein detection of HIF-1α was accomplished by processing cells in RIPA buffer (150 mM NaCl/1% IGEPAL CA-630/0.5% DOC/0.1% SDS/50 mM Tris-Cl/pH = 8.0) with Complete Mini protease cocktail (Roche Applied Science, Indianapolis, IN), followed by centrifugation (at 10,000 rpm for 20 min at 4°C) to remove cell debris. Total cellular protein (25 μg) was electrophoresed through a 4 to 12% gradient SDS-acrylamide gel, and blotted onto polyvinylidene difluoride (PVDF) membranes (300 mA, 90 min). The blot was cut horizontally in half at the 75-kD molecular weight marker and the upper half probed with monoclonal anti-HIF-1α monoclonal antibody (BD Biosciences, Franklin Lakes, NJ). The lower half of the blot was probed with mouse monoclonal anti–β-actin antibody (Sigma-Aldrich). Both were further processed using goat anti-mouse-HRP (Dako, Carpinteria, CA) as secondary antibody. Chemiluminescence was developed using Supersignal Femto Maximum Sensitivity Substrate (Pierce, Rockford, IL).

5xHRE-Luc Plasmids

A construct encoding five tandem copies of an HIF-responsive element (HRE) from the VEGF regulatory region was constructed by ligating an oligonucleotide ligand, (TCGAGCCACAGTGCATACGTGGGC TCCAACAGGTCCTCTTG and TCGACAAGAGGACCTGTTGG AGCCCACGTATGCACTGTGGC) as described previously (18), and subcloning into pGL3-Basic (Promega, Madison, WI) upstream of firefly luciferase. The CMV minimal promoter was cloned between the HRE and luciferase. The identity of the resulting construct was confirmed by DNA sequencing, and the plasmid transfected into HT29 cells in 10-cm plates using Lipofectamine 2000 (Invitrogen) or electroporated (260 mV, 1,050 μF). Cells were trypsinized 24 hours later, divided onto twelve 12-mm Transwell filters, and grown to confluence. The transfection and cell monolayer preparation was performed in a fashion such that each filter contained similar numbers of transfected cells. Luciferase activity was measured after a minimum of 24 hours under well-oxygenated or oxygen-restricted conditions. Cells from each filter were lysed in 100 μl of Glo-Lysis buffer (Promega), and luciferase activity measured in triplicate (multiwell luminometer; Harta Instruments, Gaithersburg, MD) using the Bright-Glo reagent (Promega). The total protein concentration from each filter was measured (Pierce BCA protein assay kit). Relative light units were presented per μg total protein. Each study was performed at least three times (each individual experiment with six sets each of A/L and L/L samples).

CFTR Western Blotting

Cells were lysed in RIPA buffer (150 mM NaCl/1% IGEPAL CA-630/ 0.5% DOC/0.1% SDS/50 mM Tris-Cl/pH = 8.0) containing Complete Mini protease cocktail and total protein concentration was measured. Total cell lysates at the amounts indicated were analyzed by 6% SDS-PAGE. After electroblotting onto PVDF membranes (Bio-Rad, Hercules, CA), CFTR was probed with mouse monoclonal anti-NBD1 antibody 10B6.2. The blot was otherwise processed and developed as described above. Identical samples were probed using anti–β-actin antibody as a control. Densitometry was performed using the ImageJ (http://rsb.info.nih.gov/ij/) program. The intensity of CFTR bands was normalized to β-actin.

Transepithelial Transport Measurements

Filters were mounted in an Ussing chamber (Jim's Instrument Mfg. Co., Iowa City, IA) for short-circuit current (I_{sc}) analysis. NaCl Ringer solution (145 mM Na^+/5 mM K^+/124.8 mM Cl^-/1.2 mM Ca^{2+}/1.2 Mg^{2+}mM/25 mM HCO_3^-/4.2 mM PO_3^{4-}/10 mM glucose/pH = 7.4) was added to both the apical and basolateral sides of the monolayer, oxygenated, and maintained at 37°C. An automatic voltage clamp was used to maintain the I_{sc} across the monolayer and was continuously

monitored as described previously (18). Low-chloride Ringer (6 mM Cl^- in which 118.8 mM of Cl^- was replaced by the impermeant anion gluconate) was added to the apical surface. Forskolin (20 μM; Calbiochem, San Diego, CA) was added to both sides of the monolayer to increase cellular cAMP and activate CFTR chloride channels.

Immunocytochemistry

Polarized monolayers of HT29 cells were grown to high resistance ($> 1{,}000\ \Omega \cdot cm^2$) and maintained under oxygen-restricted conditions for 72 hours. The cells were fixed in 3% formaldehyde for 10 minutes at room temperature. Monolayers were probed with monoclonal 24-1 antibody (5 μg per milliliter; American Type Culture Collection HB-11947), which recognizes amino acids 1,477 through 1,480 of the C-terminus of CFTR, and a polyclonal antibody to ZO-1 (Invitrogen), a marker of tight junctions. Secondary antibodies conjugated to Alexa Fluor 488 and 594 (Invitrogen) were used to fluorescently visualize the proteins of interest, and the images were captured on a Leitz Orthoplan camera and microscope and prepared using IPLab software (BD Biosciences, Rockville, MD). Images shown are ×100.

Murine Total RNA Collection

Five- to 10-week-old C57Bl/6 mice were maintained in a normobaric hypoxic environment containing 10% oxygen for 7 days (19, 20). This condition offers approximately the same availability of oxygen as exposure to high altitudes (i.e., 20,000 ft yields 76 mm Hg available oxygen) (21). Mice were sedated using 10 mg/kg intraperitoneal ketamine and killed by cervical dislocation. Tissue samples for RNA analysis from lung parenchyma, small bowel, and liver were collected and immediately stabilized in RNA*later*, followed by extraction using the RNeasy mini kit (Qiagen). For total RNA extraction, tissue samples were flash frozen and pulverized in liquid nitrogen. Six mice were studied per group. Applied Biosystems Taqman Gene Expression Assay for murine CFTR (Mm 00445197_m1) was used in PCR amplification with normalization to eukaryotic 18S rRNA. Littermates maintained under normoxia were tested in parallel.

Human Lung Transplant Total RNA Collection

Approval was obtained from the University of Alabama at Birmingham Institutional Review Board for Human Use. Remnant tissues from human recipient lungs were obtained during transplant and stabilized immediately upon receipt in RNA*later* according to a modification of a previously published protocol (22). Tracheal samples were taken from both male and female subjects with end-stage hypoxemic lung disease (e.g., chronic obstructive pulmonary disease [COPD] or interstitial pulmonary fibrosis). Fresh samples from intact human tracheas were washed and examined to confirm healthy-appearing surfaces and mucosal integrity. For total RNA extraction, tissue samples were flash frozen and pulverized in liquid nitrogen followed by extraction using the RNeasy mini kit. A 2- × 2-mm portion of tissue was studied for levels of CFTR mRNA. CFTR mRNA was quantified and compared with 18S ribosomal RNA using fluorescence-based polymerase chain reaction and Taqman probes. Donor lungs without known pulmonary disease were studied in parallel. One of 11 subjects was homozygous for ΔF508 mutation; all others were non-CF. Blood oxygen levels on room air in study subjects before transplantation were less than 50 to 55 mm Hg.

RESULTS

CFTR mRNA Levels Are Repressed in Submerged Cells

We examined CFTR mRNA in submerged cells with poor oxygen availability (depth of the media ranging from 5–10 mm) or with overlying media aspirated to expose the cells to air. Fluid depths *in vitro* that exceed 0.34 mm are known to markedly impede cellular oxygen access (14, 15, 23). We began these studies using HT29 cells, which express high levels of CFTR, form electrically resistant monolayers, and are capable of vectoral Cl^- transport either submerged or with air-exposed culture (24). As indicated by CFTR-specific semiquantitative PCR (Figure 1A), steady-state levels of CFTR mRNA were much lower for submerged (*lane 1*) compared with air-exposed cells (*lane 3*). When apical medium in submerged culture was removed and switched to an air interface for 24 hours (*lane 2*) or when air-exposed culture was placed under liquid for 24 hours (*lane 4*), CFTR expression patterns were reversed. Control mRNAs such as β-actin and GAPDH were not altered, indicating specificity of the findings for CFTR. Figure 1B provides relative quantification of CFTR mRNA by fluorescence-based real-time PCR. CFTR mRNA was on average 15-fold higher in air-exposed HT29 samples. We hypothesized that the hypoxic state conferred by the apical liquid layer was responsible for this phenomenon.

Liquid-Submerged Culture Is Hypoxic

We verified that fluid depth conferred a hypoxic state by three independent assays. First, we showed that HIF-1α (a protein post-translationally elevated in hypoxic cells) is increased in submerged cell cultures (Figure 2A, representative of three repeat experiments). Second, an HRE was shown to be activated by submerged compared with air-exposed cells as judged by increases in HRE-driven luciferase activity (Figure 2B). This result indicates functional enhancement of the hypoxia response via HIF after L/L treatment. Third, we used gene chip mRNA profiling to screen for hypoxia-related transcriptional effects. Figure 2C depicts a log scale scatter plot of genes differentially expressed under air-exposed versus submerged conditions from one array. Array experiments were repeated using three additional sets of samples with similar results (*see* GEO series GSE9234, http://www.ncbi.nlm.nih.gov/geo/). The mRNAs of a number of well-established hypoxia-induced marker genes such as VEGF (3), carbonic anhydrase IX (CA9) (25, 26), and fructose-biphosphate aldolase C (ALDOC) (27) were highly up-regulated (Figure 2D) under submerged conditions. CFTR mRNA was among the most strongly repressed. This finding is compatible with the data shown in Figure 1B. As expected, HIF-1α mRNA was not significantly increased after oxygen restriction (HIF-1α is increased by hypoxia post-translationally due to protein stabilization and increased protein half-life).

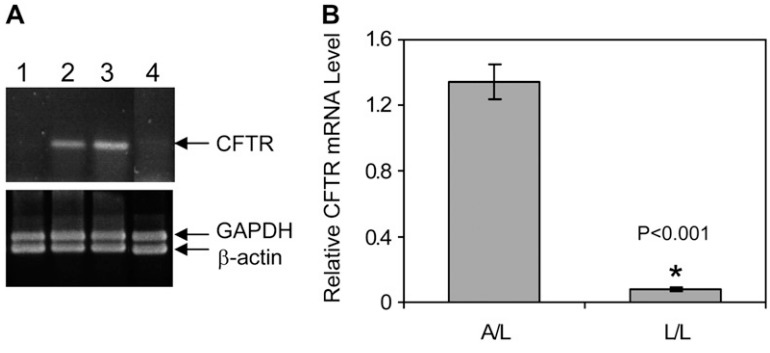

Figure 1. Effects of air exposure on cystic fibrosis transmembrance conductance regulator (CFTR) mRNA. (*A*) Semiquantitative CFTR-specific RT-PCR. HT29 total RNA samples from *lane 1*: cells submerged (48 h); *lane 2*: cells submerged for 24 hours followed by air exposure for an additional 24 hours; *lane 3*: air exposure (48 h); *lane 4*: air exposure for 24 hours, followed by cells submerged for an additional 24 hours. RT-PCR of GAPDH and β-actin mRNAs were used as internal controls in each reaction. This experiment has been reproduced nine times with very similar results. (*B*) Relative CFTR mRNA levels in HT29 cells under air-exposed or submerged conditions by real-time PCR relative quantification method ($n = 4$).

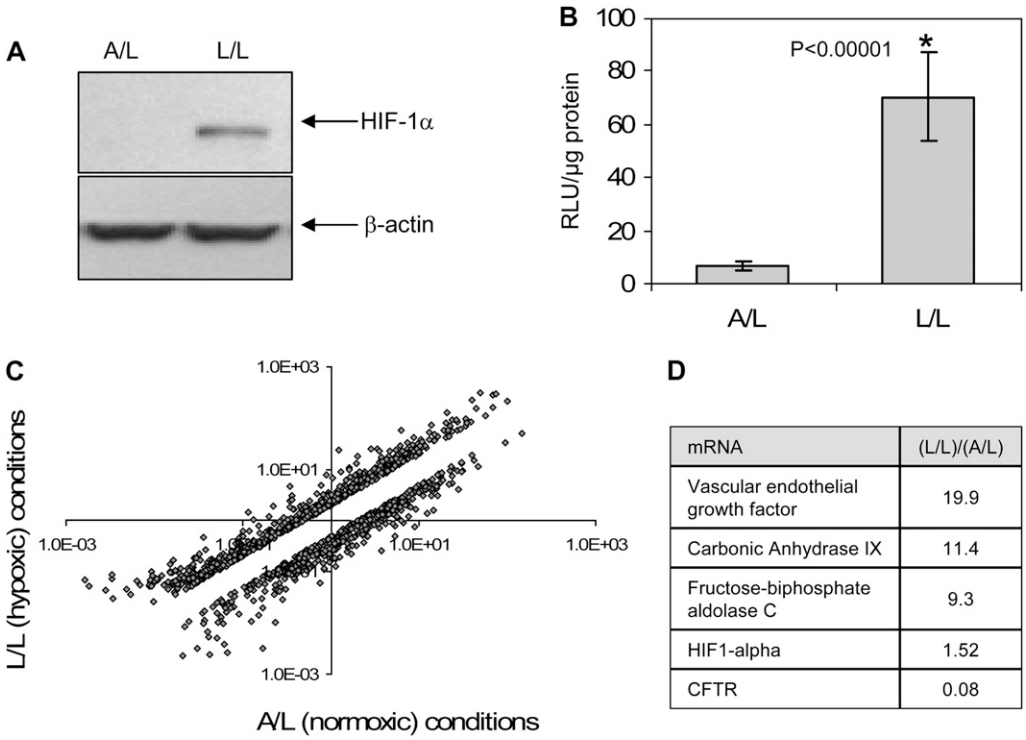

mRNA	(L/L)/(A/L)
Vascular endothelial growth factor	19.9
Carbonic Anhydrase IX	11.4
Fructose-biphosphate aldolase C	9.3
HIF1-alpha	1.52
CFTR	0.08

Figure 2. Oxygen is restricted in submerged cell monolayers. (*A*) Immunoblot showing elevation of HIF-1α under L/L compared with A/L in HT29 cell lysates. β-actin blot is shown as an internal control. This experiment was repeated three times with very similar results. (*B*) Relative luciferase activity (RLU (relative light units); light units measured/ μg total protein) in HT29 cells transfected with 5xHRE-Luc and cultured under air-exposed (A/L) or submerged (L/L) conditions ($n = 6$). All data are normalized to total cellular protein. This experiment was repeated three times with very similar results. (*C*) Comparison of global changes in HT29 mRNA under L/L versus A/L conditions. Unique genes that were differentially expressed 2-fold or greater are shown on the *log scale scatter plot* (*see* GEO series GSE9234 for raw data). *Upper clouds* indicate transcripts at increased levels under air and *lower clouds* indicate transcripts decreased under L/L (cells submerged). (*D*) Relative mRNA levels of known genes for hypoxic signaling (VEGF, CA9, ALDOC) were substantially changed. The data show mRNA ratios of indicated genes from a representative array; results were similar from four repeat array studies.

CFTR Protein Is Repressed in a Reversible Fashion in Submerged Cells

We next investigated effects on protein expression by Western blot analysis. Steady-state CFTR significantly decreased in submerged cells (Figure 3A, *lane 2*) compared with air-exposed cells (Figure 3A, *lane 1*). By densitometry, CFTR protein in L/L samples was decreased by 80 to 90% compared with A/L. This decrease in CFTR was fully recovered upon removing the overlying liquid medium for 48 hours (Figure 3A, *lane 3*). β-actin protein levels in the same samples appeared similar (Figure 3A, *lower panel*). These data therefore further support the assertion that CFTR protein repression does not result from a global effect on cellular mRNA or protein (*see also* Figures 1A [GAPDH and β-actin controls], 2C, and 2D [genome-wide analysis]). Resistance of cell monolayers was measured after L/L incubation and was stable and similar irrespective of air or L/L exposure, indicating integrity of the samples (data not shown). When CFTR was visualized by confocal microscopy, HT29 cells showed abundant overall CFTR protein under A/L (Figure 3B). When cells were submerged, CFTR protein levels were much lower (Figure 3B).

Hypoxia and Hypoxia Mimetics Impair CFTR mRNA, Protein, and Function

To further investigate hypoxic signaling for effects on CFTR mRNA, quantitative PCR was performed with cells in a sealed hypoxia chamber (1% oxygen) or after treatment with well-established pharmacologic activators of hypoxic signaling, DMOG and $CoCl_2$ (28, 29) (Figure 4A). To demonstrate that these findings are not confined to a single epithelial type, experiments were also performed in human pulmonary cells (Calu-3) (24). Overlying fluid depths reaching 5 to 10 mm (analogous to L/L conditions) are observed as a result of mucus plugging in diseases such as cystic fibrosis. CFTR mRNA

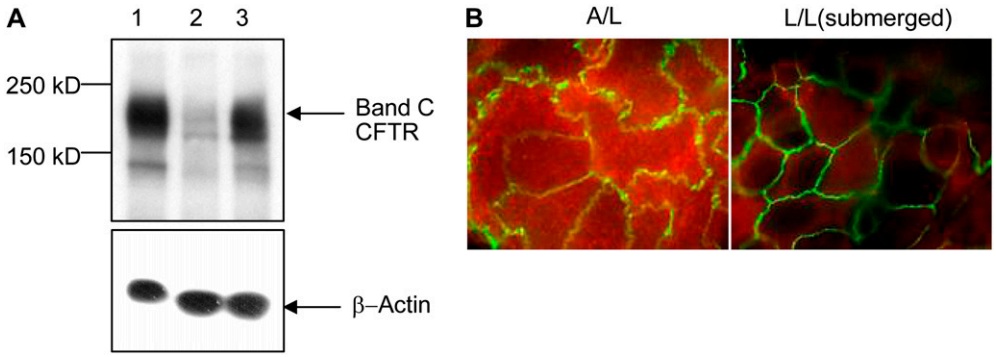

Figure 3. CFTR protein level is lower in cells cultured under L/L. (*A*) Western blot of HT29 cell lysates (40 μg total protein per lane). *Upper panel* shows mature band C form of CFTR in A/L (*lane 1*) or L/L (*lane 2*) conditions. In *lane 3*, HT29 cells were first submerged (L/L) for 48 hours followed by air exposure for an additional 48 hours. The *lower panel* depicts an identical blot probed with β-actin antibody as a control. This experiment was repeated three times with very similar results. A representative blot is shown. (*B*) CFTR is shown by red fluorescence in a confocal *en face* section of the apical plasma membrane (*original magnification*: ×100) of HT29 cells. ZO-1 (a marker of tight junctions) is depicted by green fluorescence at cellular margins.

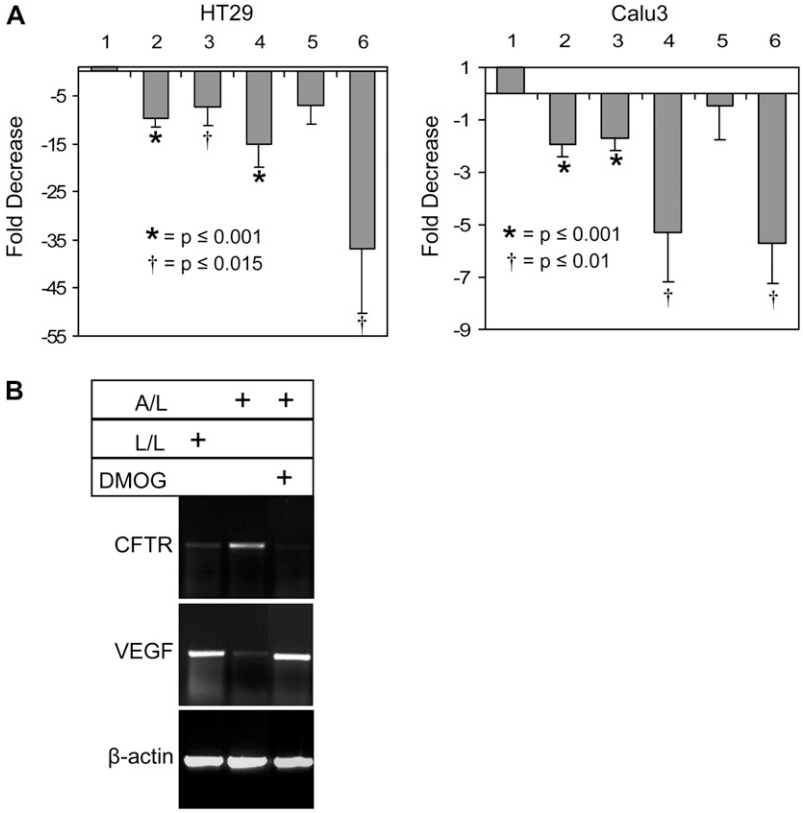

Figure 4. Repression of CFTR by hypoxia and the hypoxia mimetic, DMOG. (*A*) Changes in CFTR mRNA normalized to 18S rRNA in HT29 and Calu3 cells. Fold difference is in comparison to *lane 1* + SEM. *Lane 1*: A/L; *lane 2*: L/L; *lane 3*: A/L with 100 μM $CoCl_2$; *lane 4*: A/L with 2 mM DMOG; *lane 5*, A/L with 1% O_2, 5% CO_2, 94% N_2; *lane 6*, L/L with 1% O_2, 5% CO_2, 94% N_2. For HT29, $n = 3$ ($CoCl_2$) or 6 to 8 (all other conditions) filters per condition; for Calu3, $n = 4$ filters per condition). Statistics are shown in comparison to A/L. + SEM. (*B*) CFTR or VEGF semiquantitative RT-PCR from HT29 total RNA. *Lane 1*: L/L; *lane 2*: A/L; *lane 3*: A/L, 2 mM DMOG treated overnight. This experiment was repeated three times with very similar results. A representative gel is shown.

expression was repressed at low concentrations of ambient oxygen (Figure 4A, *lanes 2*, *5*, and *6*); a result confirming a causal link between poor oxygen availability and diminished CFTR. Cells cultured at an air interface in the presence of the hypoxia mimetics DMOG (2 mM) or $CoCl_2$ (100 μM) also exhibited CFTR repression (Figure 4A, *lanes 3* and *4*).

DMOG is a 2-oxoglutarate–dependent dioxygenase inhibitor that stabilizes HIF-1α by blocking degradation (28, 30) and is commonly employed as a hypoxia mimetic. The compound also inhibits Factor Inhibiting HIF (FIH), an asparaginyl hydroxylase, which further augments the HIF response (31). Gene expression patterns induced by hypoxia and by DMOG are known to be similar (32). We therefore investigated CFTR under DMOG-induced hypoxia-like conditions. Semiquantitative PCR (Figure 4B) indicated strong suppression of CFTR mRNA after DMOG treatment in air-exposed HT29 cells. VEGF mRNA (a hypoxia marker) varied inversely in relation to CFTR.

Figure 5A indicates that CFTR protein levels are decreased in 2 mM DMOG-treated colonic (HT29) and pulmonary (Calu3) cells. As shown in Figure 5B, both HT29 and Calu-3 monolayers grown at an air interface exhibited robust forskolin-activated CFTR channel activity. However, when cells were cultured under A/L conditions, treatment with DMOG for 24 hours inhibited the chloride transport stimulated by forskolin (a CFTR activator) by 60% (HT29) or 92% (Calu-3) compared with controls. Similar conclusions were reached with the hypoxia mimetic desferrioxamine (data not shown). Taken together, these results demonstrate that signaling pathways elicited by low oxygen can strongly down-regulate steady-state levels of CFTR mRNA, protein, and transepithelial transport. The extent to which a 6- to 17-fold repression of CFTR mRNA (induced by DMOG) can fully account for effects observed here will require further study, particularly in light of the large number of individual mRNAs altered by hypoxia (Figure 2C).

Low Oxygen Represses CFTR mRNA in Murine and Human Tissues *In Vivo*

To further examine the impact of oxygen availability on CFTR mRNA, we obtained organs from mice chronically exposed to hypoxia. Because a previous study demonstrated that exposure to 7% oxygen for as little as 60 minutes induced hypoxic signaling in rat brain, lung, and kidney tissues *in vivo* (33), we selected this as a working exposure level. CFTR mRNA in chronically hypoxic mice was approximately 50% lower in trachea and airways, gastrointestinal tract, and liver samples than in normoxic animals (for specificity, all data was derived from a similar amount of tissue starting material and was normalized to 18S ribosomal RNA [Figure 6A]). We also investigated CFTR mRNA in tracheal tissue samples from human recipient lungs at the time of transplantation ($n = 11$ from each group). Although patients with end-stage lung disease are placed on supplemental oxygen before transplantation, mucus accumulation in the airways impedes oxygen access to surface epithelial cells (2), and serosal O_2 delivery is markedly repressed due to hypoxemia. CFTR expression in freshly excised airway tissues after lung excision and donor (normoxic) lung transplantation samples (no underlying pulmonary disease) were studied as paired controls in an otherwise identical manner (Figure 6B).

DISCUSSION

In this report, we show that hypoxia contributes to reduction of cell surface CFTR by decreasing steady-state CFTR mRNA. Bebok and coworkers (34) previously demonstrated that poor cellular oxygenation leads to CFTR protein instability and degradation in a canine cell line, although the involvement of CFTR mRNA regulation was not implicated. The present studies provide a formal mRNA analysis, normalization to

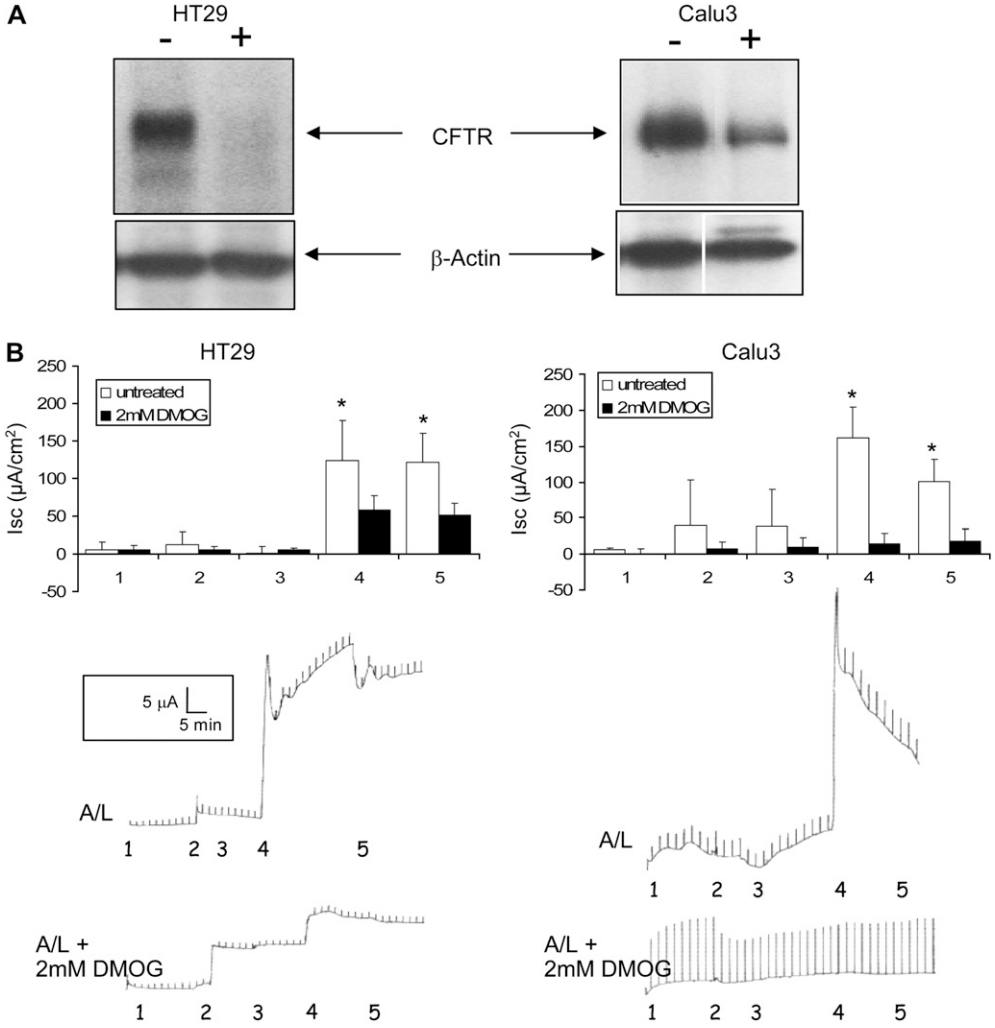

Figure 5. Hypoxia mimetic DMOG impairs CFTR function. (*A*) Western blot of CFTR and β-actin in HT-29 (*left*) and Calu3 (*right*) cells after 2 mM DMOG treatment for 48 hours. This experiment was performed three times with very similar results. A representative blot is shown. By densitometry, protein levels were reduced by approximately 90% in HT29 and 50% in Calu3 cells. (*B*) Short-circuit current (I_{sc}) as measured by μA/cm² upon stimulation with forskolin (an activator of CFTR chloride channel function) in HT29 (*left*) and Calu3 (*right*) cell monolayers (transepithelial resistances > 1,000 Ω·cm²). A/L cultures are shown without or with 2 mM DMOG for 24 hours. *Top*: Summary data, n = 8–10 filters per condition. *Bottom*: representative tracings. 1 = regular Ringer both sides; 2 = replacement of apical Ringer with low (6 mM) Cl^- Ringer (low chloride solution); 3 = 500 s after addition of low chloride; 4 = addition of 20 μM forskolin to apical and basolateral sides; 5 = 1,000 s after addition of forskolin. *P < 0.0003. HT-29 and Calu3 cells have robust responses to forskolin that are known to be CFTR dependent and lack amiloride-sensitive currents. DMOG at 1 to 2 mM is tolerated, and did not alter transepithelial resistance of the monolayers. Higher concentrations of DMOG become toxic after 48 hours of incubation with Calu3 cells.

housekeeping mRNAs, and comparison with known hypoxia-responsive genes in human cells. The findings establish that impaired cellular oxygenation can dramatically suppress steady-state CFTR mRNA in HT29 and Calu3 cells. These effects were shown using liquid cell submergence, restriction of ambient oxygen, hypoxia mimetic agents such as $CoCl_2$ or DMOG, and *in vivo* oxygen deprivation. The results support a robust regulatory mechanism suppressing CFTR mRNA.

Gene expression patterns induced by hypoxia and DMOG are similar (32), and DMOG is commonly used in experimental settings to mimic hypoxia. Our finding that DMOG impairs transepithelial Cl^- transport in airway epithelia (Figure 5) is explained in part by suppression of CFTR mRNA (Figure 4) compared with control mRNAs such as 18S (Figure 4A) or β-actin (Figure 4B). Importantly, these studies establish that routine CFTR tissue culture with overlying liquid media can impair levels of CFTR mRNA, a finding that has not been appreciated in the past. The studies with DMOG and $CoCl_2$ also suggest that HIF-1α might contribute to inhibition of CFTR mRNA, although further experiments will be necessary to investigate this possibility.

Many patients with CF have disease attributable to defects in mRNA production or stability (e.g., nonsense-mediated decay), or due to levels of CFTR at the cell surface inadequate to

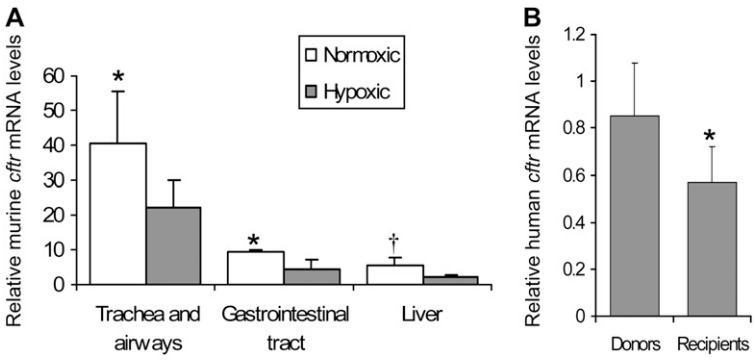

Figure 6. Hypoxia down-regulates CFTR mRNA *in vivo*. (*A*) Relative quantitation of CFTR mRNA in different organs of C57Bl/6 mice + SEM (n = 8 animals per condition) (*P < 0.05; †P = 0.057). (*B*) Relative quantitation of CFTR mRNA from human donor and recipient tracheas at time of transplantation. Mean donor and recipient RNA levels are shown + SEM; *P = 0.030 (n = 11 tracheas per condition).

forestall pulmonary decline (1). In contrast to healthy human subjects, in whom 5 to 10% of normal CFTR has been estimated to prevent a CF phenotype (35, 36), virtually nothing is known regarding the amount of CFTR mRNA (or protein) necessary to stabilize lung disease in severely compromised, rapidly deteriorating individuals with the disease. It is generally believed that patients with CF exist along a continuum from completely absent CFTR to a level of activity adequate for near-normal pulmonary physiology. For example, the A455E mutation results in marginally reduced function of CFTR and clinically mild pulmonary disease, a later age at diagnosis, and a substantially improved prognosis (37). Even classically severe mutations (e.g., the common ΔF508 allele) have been reported by some (but not all) groups to retain low-level function in humans and mice *in vivo* (38–42). If residual CFTR mRNA, protein, and function serve to slow CF pulmonary decline, it is reasonable to imagine that repression of CFTR by low oxygen could contribute to respiratory failure in the disease.

In chronic inflammatory diseases such as COPD and CF, impaired mucociliary clearance promotes infection and inflammation, and results in regional hypoxia in airway epithelia. In an earlier study, Worlitzsch and colleagues measured pO_2 directly from bronchi of chronically infected patients with CF, and noted a value of 180 mm Hg (consistent with supplemental oxygen administered during bronchoscopy). However, oxygen declined sharply to a mean value of 2.5 mm Hg when measured in mucopurulent material obstructing the lobar bronchus and airway epithelium (2). It was also suggested that bacterial oxygen consumption in the airways would markedly exacerbate local hypoxia, resulting in a near anoxic situation even in the setting of supplemental O_2. When we examined murine tissues exposed to hypoxic conditions, or pulmonary tissues from hypoxemic individuals with respiratory failure, CFTR mRNA was significantly repressed.

There is growing appreciation of the ways genetic or environmental factors might "tip the balance" toward CF pulmonary decompensation. In ΔF508 homozygous patients, altered expression of TGF-β confers a significantly worse pulmonary outcome (43, 44). In subjects with CF with forced expiratory volume per second (FEV_1) in the range of 40 to 70%, unpredictable swings in pulmonary functional capacity are commonly observed, including bouts of severe clinical deterioration. The tenuous clinical balance may be influenced by impairment of CFTR from environmental insults such as inflammation or cigarette smoke (34, 45, 46). Changes in CFTR mRNA due to hypoxia (Figures 1–3), together with post-transcriptional loss of CFTR maturation (decrease up to 50-fold in low oxygen [45]), and globally impaired mRNA utilization due to low oxygen (47, 48), would therefore be expected to accelerate pulmonary failure in marginally compensated individuals with CF.

Maintenance of normal cell function during hypoxia depends on the ability of cells to develop adaptive strategies that overcome O_2 deprivation. Cells adjust to hypoxia by decreasing energy utilization in the setting of limited oxidative phosphorylation, and oxygen sensing down-regulates ATP consumption throughout the hypoxic cell environment (50). Vectoral ion transport is known to require substantial energy expenditure, and is typically suppressed during hypoxic stress as a means of conserving energy. For example, activity of Na^+, K^+-ATPase decreases by up to about 75% during oxygen restriction (51). Similarly, expression of the Na^+, K^+ ATPase and all subunits of the epithelial Na^+ channel are reversibly repressed in both a time- and oxygen-dependent manner by low O_2 (52). Because vectoral Cl^- transport through CFTR is an energy-dependent process, it is reasonable to imagine that this pathway might also be down-regulated during hypoxia. Having said this, different tissue and cell types may vary in responsiveness to low oxygen. For example, Zaidi and coworkers (53) provided evidence that hypoxic conditions in the cornea exacerbated binding and internalization of *P. aeruginosa* and augmented CFTR expression at the cell surface. These earlier studies, however, used milder oxygen restriction than studied here (15% ambient O_2). It remains possible, however, that CFTR expression is differentially regulated in the cornea depending on the extent of oxygen deprivation.

A recent report demonstrated 60% loss of CFTR mRNA in a subset of mountaineers exposed to hypoxia at high altitude (49), and recent clinical experiments have shown *in vivo* CFTR ion transport defects attributable to chronic smoking (9). Hypoxemia (low blood oxygen content), *per se*, would not be anticipated to elicit CFTR deficiency in lung epithelium because of the dual oxygen supply to pulmonary tissues (from both blood and the airways themselves). However, mucus production completely buries extensive segments of the pulmonary surface in diseases such as CF, COPD, and asthma. Thick layers of mucus plastered to large regions of the lung are known to abrogate oxygen delivery. The present studies therefore point to local hypoxia and acquired CFTR mRNA deficiency as potential contributors to mucus obstruction, bronchiectasis, and pulmonary injury in the clinical setting, including both inherited (cystic fibrosis) and other, more common obstructive pulmonary diseases.

Conflict of Interest Statement: None of the authors has a financial relationship with a commercial entity that has an interest in the subject of this manuscript

Acknowledgments: The authors thank Ms. Carolyn Cox and Mrs. Jenny Mott for help preparing the manuscript.

References

1. Rowe SM, Miller S, Sorscher EJ. Cystic fibrosis. *N Engl J Med* 2005;352: 1992–2001.
2. Worlitzsch D, Tarran R, Ulrich M, Schwab U, Cekici A, Meyer KC, Birrer P, Bellon G, Berger J, Weiss T, *et al*. Effects of reduced mucus oxygen concentration in airway *Pseudomonas* infections of cystic fibrosis patients. *J Clin Invest* 2002;109:317–325.
3. Semenza GL. Involvement of hypoxia-inducible factor 1 in pulmonary pathophysiology. *Chest* 2005;128:592S–594S.
4. Semenza GL. Pulmonary vascular responses to chronic hypoxia mediated by hypoxia-inducible factor 1. *Proc Am Thorac Soc* 2005;2:68–70.
5. Kwapiszewska G, Wilhelm J, Wolff S, Laumanns I, Koenig IR, Ziegler A, Seeger W, Bohle RM, Weissmann N, Fink L. Expression profiling of laser-microdissected intrapulmonary arteries in hypoxia-induced pulmonary hypertension. *Respir Res* 2005;6:109.
6. Tong Q, Zheng L, Lin L, Li B, Wang D, Huang C, Li D. VEGF is upregulated by hypoxia-induced mitogenic factor via the PI-3K/Akt-NF-kappaB signaling pathway. *Respir Res* 2006;7:37.
7. Jain M, Sznajder JI. Effects of hypoxia on the alveolar epithelium. *Proc Am Thorac Soc* 2005;2:202–205.
8. Yu AY, Frid MG, Shimoda LA, Wiener CM, Stenmark K, Semenza GL. Temporal, spatial, and oxygen-regulated expression of hypoxia-inducible factor-1 in the lung. *Am J Physiol* 1998;275:L818–L826.
9. Cole LA, Scheid JM, Tannen RL. Induction of mitochondrial metabolism and pH-modulated ammoniagenesis by rocking LLC-PK1 cells. *Am J Physiol* 1986;251:C293–C298.
10. Dickman KG, Mandel LJ. Glycolytic and oxidative metabolism in primary renal proximal tubule cultures. *Am J Physiol* 1989;257: C333–C340.
11. Nowak G, Schnellmann RG. Improved culture conditions stimulate gluconeogenesis in primary cultures of renal proximal tubule cells. *Am J Physiol* 1995;268:C1053–C1061.
12. Ohno K, Maier P. Cultured rat hepatocytes adapt their cellular glycolytic activity and adenylate energy status to tissue oxygen tension: influences of extracellular matrix components, insulin and glucagon. *J Cell Physiol* 1994;160:358–366.

13. Sahai A, Cole LA, Clarke DL, Tannen RL. Rocking promotes differentiated properties in LLC-PK cells by improved oxygenation. *Am J Physiol* 1989;256:C1064–C1069.
14. Stevens KM. Oxygen requirements for liver cells *in vitro*. *Nature* 1965; 206:199.
15. Werrlein RJ, Glinos AD. Oxygen microenvironment and respiratory oscillations in cultured mammalian cells. *Nature* 1974;251:317–319.
16. Dorris DR, Ramakrishnan R, Trakas D, Dudzik F, Belval R, Zhao C, Nguyen A, Domanus M, Mazumder A. A highly reproducible, linear, and automated sample preparation method for DNA microarrays. *Genome Res* 2002;12:976–984.
17. Ramakrishnan R, Dorris D, Lublinsky A, Nguyen A, Domanus M, Prokhorova A, Gieser L, Touma E, Lockner R, Tata M, *et al*. An assessment of Motorola CodeLink microarray performance for gene expression profiling applications. *Nucleic Acids Res* 2002;30:e30.
18. Venglarik CJ, Dawson DC. Cholinergic regulation of Na absorption by turtle colon: role of basolateral K conductance. *Am J Physiol* 1986; 251:C563–C570.
19. Chen YF, Feng JA, Li P, Xing D, Ambalavanan N, Oparil S. Atrial natriuretic peptide-dependent modulation of hypoxia-induced pulmonary vascular remodeling. *Life Sci* 2006;79:1357–1365.
20. Chen YF, Feng JA, Li P, Xing D, Zhang Y, Serra R, Ambalavanan N, Majid-Hassan E, Oparil S. Dominant negative mutation of the TGF-beta receptor blocks hypoxia-induced pulmonary vascular remodeling. *J Appl Physiol* 2006;100:564–571.
21. Arthur C, Hall JE. Textbook of medical physiology, 10th ed. Ch. 43: aviation, high-altitude, and space physiology. Philadelphia: W. B. Saunders Company; 2000. pp. 496–498.
22. Ruiz FE, Clancy JP, Perricone MA, Bebok Z, Hong JS, Cheng SH, Meeker DP, Young KR, Schoumacher RA, Weatherly MR, *et al*. A clinical inflammatory syndrome attributable to aerosolized lipid-DNA administration in cystic fibrosis. *Hum Gene Ther* 2001;12:751–761.
23. Ostrowski LE, Nettesheim P. Inhibition of ciliated cell differentiation by fluid submersion. *Exp Lung Res* 1995;21:957–970.
24. Gruenert DC, Willems M, Cassiman JJ, Frizzell RA. Established cell lines used in cystic fibrosis research. *J Cyst Fibros* 2004;3:191–196.
25. Ivanov S, Liao SY, Ivanova A, Danilkovitch-Miagkova A, Tarasova N, Weirich G, Merrill MJ, Proescholdt MA, Oldfield EH, Lee J, *et al*. Expression of hypoxia-inducible cell-surface transmembrane carbonic anhydrases in human cancer. *Am J Pathol* 2001;158:905–919.
26. Potter C, Harris AL. Hypoxia inducible carbonic anhydrase IX, marker of tumour hypoxia, survival pathway and therapy target. *Cell Cycle* 2004;3:164–167.
27. Jean JC, Rich CB, Joyce-Brady M. Hypoxia results in an HIF-1-dependent induction of brain-specific aldolase C in lung epithelial cells. *Am J Physiol Lung Cell Mol Physiol* 2006;291:L950–L956.
28. Ivan M, Haberberger T, Gervasi DC, Michelson KS, Gunzler V, Kondo K, Yang H, Sorokina I, Conaway RC, Conaway JW, *et al*. Biochemical purification and pharmacological inhibition of a mammalian prolyl hydroxylase acting on hypoxia-inducible factor. *Proc Natl Acad Sci USA* 2002;99:13459–13464.
29. Yuan Y, Hilliard G, Ferguson T, Millhorn DE. Cobalt inhibits the interaction between hypoxia-inducible factor-alpha and von Hippel-Lindau protein by direct binding to hypoxia-inducible factor-alpha. *J Biol Chem* 2003;278:15911–15916.
30. Asikainen TM, Schneider BK, Waleh NS, Clyman RI, Ho WB, Flippin LA, Gunzler V, White CW. Activation of hypoxia-inducible factors in hyperoxia through prolyl 4-hydroxylase blockade in cells and explants of primate lung. *Proc Natl Acad Sci USA* 2005;102:10212–10217.
31. Koivunen P, Hirsila M, Gunzler V, Kivirikko KI, Myllyharju J. Catalytic properties of the asparaginyl hydroxylase (FIH) in the oxygen sensing pathway are distinct from those of its prolyl 4-hydroxylases. *J Biol Chem* 2004;279:9899–9904.
32. Elvidge GP, Glenny L, Appelhoff RJ, Ratcliffe PJ, Ragoussis J, Gleadle JM. Concordant regulation of gene expression by hypoxia and 2-oxoglutarate-dependent dioxygenase inhibition: the role of HIF-1alpha, HIF-2alpha, and other pathways. *J Biol Chem* 2006;281:15215–15226.
33. Wiener CM, Booth G, Semenza GL. In vivo expression of mRNAs encoding hypoxia-inducible factor 1. *Biochem Biophys Res Commun* 1996;225:485–488.
34. Bebok Z, Varga K, Hicks JK, Venglarik CJ, Kovacs T, Chen L, Hardiman KM, Collawn JF, Sorscher EJ, Matalon S. Reactive oxygen nitrogen species decrease cystic fibrosis transmembrane conductance regulator expression and cAMP-mediated Cl- secretion in airway epithelia. *J Biol Chem* 2002;277:43041–43049.
35. Amaral MD. Processing of CFTR: traversing the cellular maze–how much CFTR needs to go through to avoid cystic fibrosis? *Pediatr Pulmonol* 2005;39:479–491.
36. Ramalho AS, Beck S, Meyer M, Penque D, Cutting GR, Amaral MD. Five percent of normal cystic fibrosis transmembrane conductance regulator mRNA ameliorates the severity of pulmonary disease in cystic fibrosis. *Am J Respir Cell Mol Biol* 2002;27:619–627.
37. De Braekeleer M, Allard C, Leblanc JP, Simard F, Aubin G. Genotype-phenotype correlation in cystic fibrosis patients compound heterozygous for the A455E mutation. *Hum Genet* 1997;101:208–211.
38. Bronsveld I, Mekus F, Bijman J, Ballmann M, de Jonge HR, Laabs U, Halley DJ, Ellemunter H, Mastella G, Thomas S, *et al*. Chloride conductance and genetic background modulate the cystic fibrosis phenotype of Delta F508 homozygous twins and siblings. *J Clin Invest* 2001;108:1705–1715.
39. Drumm M. What happens to deltaF508 in vivo? *J Clin Invest* 1999;103: 1369–1370.
40. Kalin N, Claass A, Sommer M, Puchelle E, Tummler B. DeltaF508 CFTR protein expression in tissues from patients with cystic fibrosis. *J Clin Invest* 1999;103:1379–1389.
41. Kelley TJ, Al-Nakkash L, Cotton CU, Drumm ML. Activation of endogenous deltaF508 cystic fibrosis transmembrane conductance regulator by phosphodiesterase inhibition. *J Clin Invest* 1996;98:513–520.
42. Kelley TJ, Thomas K, Milgram LJ, Drumm ML. In vivo activation of the cystic fibrosis transmembrane conductance regulator mutant deltaF508 in murine nasal epithelium. *Proc Natl Acad Sci USA* 1997; 94:2604–2608.
43. Arkwright PD, Laurie S, Super M, Pravica V, Schwarz MJ, Webb AK, Hutchinson IV. TGF-beta(1) genotype and accelerated decline in lung function of patients with cystic fibrosis. *Thorax* 2000;55:459–462.
44. Drumm ML, Konstan MW, Schluchter MD, Handler A, Pace R, Zou F, Zariwala M, Fargo D, Xu A, Dunn JM, *et al*. Genetic modifiers of lung disease in cystic fibrosis. *N Engl J Med* 2005;353:1443–1453.
45. Bebok Z, Tousson A, Schwiebert LM, Venglarik CJ. Improved oxygenation promotes CFTR maturation and trafficking in MDCK monolayers. *Am J Physiol Cell Physiol* 2001;280:C135–C145.
46. Cantin AM, Hanrahan JW, Bilodeau G, Ellis L, Dupuis A, Liao J, Zielenski J, Durie P. Cystic fibrosis transmembrane conductance regulator function is suppressed in cigarette smokers. *Am J Respir Crit Care Med* 2006;173:1139–1144.
47. Koritzinsky M, Magagnin MG, van den Beucken T, Seigneuric R, Savelkouls K, Dostie J, Pyronnet S, Kaufman RJ, Weppler SA, Voncken JW, *et al*. Gene expression during acute and prolonged hypoxia is regulated by distinct mechanisms of translational control. *EMBO J* 2006;25:1114–1125.
48. van den Beucken T, Koritzinsky M, Wouters BG. Translational control of gene expression during hypoxia. *Cancer Biol Ther* 2006;5:749–755.
49. Mairbaurl H, Schwobel F, Hoschele S, Maggiorini M, Gibbs S, Swenson ER, Bartsch P. Altered ion transporter expression in bronchial epithelium in mountaineers with high-altitude pulmonary edema. *J Appl Physiol* 2003;95:1843–1850.
50. Hochachka PW, Buck LT, Doll CJ, Land SC. Unifying theory of hypoxia tolerance: molecular/metabolic defense and rescue mechanisms for surviving oxygen lack. *Proc Natl Acad Sci USA* 1996;93:9493–9498.
51. Buck LT, Hochachka PW. Anoxic suppression of Na(+)-K(+)-ATPase and constant membrane potential in hepatocytes: support for channel arrest. *Am J Physiol* 1993;265:R1020–R1025.
52. Clerici C, Matthay MA. Hypoxia regulates gene expression of alveolar epithelial transport proteins. *J Appl Physiol* 2000;88:1890–1896.
53. Zaidi T, Mowrey-McKee M, Pier GB. Hypoxia increases corneal cell expression of CFTR leading to increased Pseudomonas aeruginosa binding, internalization, and initiation of inflammation. *Invest Ophthalmol Vis Sci* 2004;45:4066–4074.